Vibrational state distribution of Na_2^+-ions created in ultracold collisions

J.J. Blangé, J.M. Zijlstra, A. Amelink, X. Urbain*, H. Rudolph, P. van der Straten, H.C.W. Beijerinck and H.G.M. Heideman

Debye Institute, Department of Atomic- and Interface Physics,
Utrecht University, P.O. Box 80.000, 3508 TA Utrecht, The Netherlands
(accepted by Phys. Rev. Lett.)

The vibrational distribution $P(v)$ of Na_2^+ ions created in ultracold collisions in a magneto-optical trap has been determined. Only two vibrational states with $v = 2$ and 3 are populated and we find $P(2)$=0.29±0.02 and $P(3)$=0.71±0.02. The results provide conclusive evidence that the ionization mechanism is photo-associative autoionization, and not photo-associative photoionization and will form a fundamental test for the theoretical description of the process.

Pacs Numbers: 33.80.Gj, 32.80.Pj, 33.80.Eh, 33.20.Tp

In recent years various groups have employed optical traps to study cold collisions at temperatures below 1 mK [1]. In most cases the collisions have been studied by observing the loss of atoms from the trap; however, in some cases the production of ions in cold collisions with alkalis has been used as a direct probe of the reactions [2]. This is possible, since in the case of Na two excited atoms have acquired enough energy to autoionize to Na_2^+ at small internuclear distance. In cold collisions the collision time is longer than the lifetime of the excited state, in which case the absorptions have to take place during the collision in two, successive excitation steps. These studies have yielded a wealth of information on the intermediate, singly excited states, since the second excitation step is believed to give no extra structure to the ionization signal [3–5]. However, the nature of the second step remained unclear. In ref. [3] direct photo-ionization of the singly excited state to the ionic continuum is discussed as the second step in their high intensity, single color experiment. This process (see Fig. 1) we will refer to as Photo-Associative Photo-Ionization (PAPI). In ref. [6] the two excitations were achieved using two colors and the intensities and frequencies of the two colors could be varied. Using energy considerations it was found, that the second excitation step was to doubly excited states of Na_2, followed by autoionization of the molecule at small internuclear distance. The same mechanism is discussed by Lett *et al.* in relation to their work on Condon oscillations in the continuum [7]. We will refer to this process as Photo-Associative Autoionization (PAAI). Although the PAPI and PAAI processes yield the same reaction products (Na_2^+ and e^-), the physics of the two ionization mechanisms is very different. Since no final state detection has been made in both experiments no definite assignment of the second step can be made.

To resolve this problem one has to analyze the reaction products. This can be done either by detecting the energy spectrum of the emitted electrons or by detecting the vibrational distribution of the produced ions. These two methods are comparable and yield similar information. The outcome of such an analysis would be very different for the PAPI process compared to the PAAI process. In the first case transitions can occur to all vibrational states which are energetically allowed and their relative populations depend on the Franck-Condon overlap between the molecular singly excited state and the electronic ground state of Na_2^+. In the PAAI process the population of the vibrational states depends on the crossing of the potential curve of the doubly excited states with the ionic ground state potential. If this crossing is energetically close to the classical turning point of the doubly excited state, it is to be expected that only one or two vibrational states are populated, since the kinetic energy is extremely small in cold collisions. An analysis of the vibrational state distribution of the formed Na_2^+-ion would therefore provide an excellent means to distinguish between the two possible mechanisms. Such an analysis could in principle be performed by measuring the kinetic distribution of the emitted electrons. However, since the emitted electrons have energies of the order of 30 meV, electron energy detection in an optical trap with large external fields (optical, magnetic) is not easily realized.

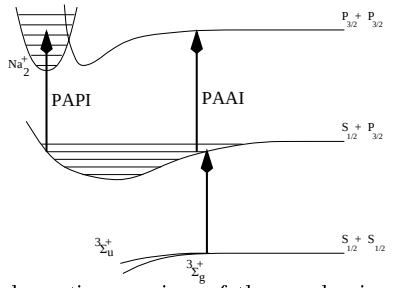

FIG. 1. Schematic overview of the mechanisms leading to molecular ion formation in cold collisions of excited Na atoms.

In this work we report on the first determination of the vibrational state distribution $P(v)$ in Na_2^+ ions produced in ultracold collisions. For the cooling and trapping of the atoms we use a Magneto-Optical Trap (MOT) [8]. The method applied is based on the wavelength dependent photodissociation of Na_2^+ ions:

$$\mathrm{Na}_2^+(X^2\Sigma_g^+; v, J) + h\nu \longrightarrow \mathrm{Na}_2^+(1^2\Sigma_u^+) \qquad (1)$$
$$\longrightarrow \mathrm{Na}^+ + \mathrm{Na}(3s) + \Delta E_{kin},$$

where v and J are the vibrational and rotational quantum numbers of the Na_2^+ ionic ground state, respectively, $h\nu$ is the photon energy of the dissociating laser, and ΔE_{kin} the kinetic energy of the fragments as a result of the photodissociation. Previously, this method has been successfully applied to Na_2^+ ions produced through associative ionization in collisions in thermal beams [9] and is described in detail by Blangé *et al.* [10]. Since the ions formed in the collisions are extracted from the MOT with a weak electric field to the detection chamber, the detection process does not interfere with the cooling and trapping of the atoms.

The setup for the MOT has been described before by Molenaar *et al.* [6]. Briefly, atoms are cooled and trapped from a background pressure of sodium in a vapor cell [11] to temperatures in the order of 200 μK and densities of 10^{10} atoms/cm^3. To avoid trapping of the population in the wrong hyperfine ground state during the cooling process [8], sidebands are generated on the cooling laser with an electro-optical modulator (EOM) and the two first order sidebands are used to cool and repump. The EOM frequency is 860 MHz and the first sidebands both contain 34% of the total irradiance. The cooling laser beam is split up into three counter-propagating pairs of beams that intersect at the center of the vacuum chamber filled with sodium vapor with a background pressure of $5 \cdot 10^{-8}$ Torr. Two solenoids outside the chamber generate a quadrupole magnetic field with a gradient of 20 Gauss/cm in the trap region. We observe cooling and trapping of atoms when the laser frequencies are tuned to the D_2 line of sodium ($3^2S_{1/2} \rightarrow 3^2P_{3/2}$) slightly red of the atomic hyperfine transitions $F = 2 \rightarrow F = 3$ and $F = 1 \rightarrow F = 2$ (type I MOT) or the transitions $F = 1 \rightarrow F = 0$ and $F = 2 \rightarrow F = 2$ (type II MOT), as described before [8,12]. The cooling occurs via the first transition mentioned, whereas the excitation via the second transition prevents the optical trapping of the atoms in the (wrong) $F = 1$ or $F = 2$ ground states, respectively. In the type II MOT the cloud of cold atoms is larger (about 2.5 mm diameter versus 0.3 mm for type I), whereas the density is only a factor 2 smaller. Therefore the type II MOT produces more Na_2^+ ions (≈80 times) than the type I MOT. The measurements reported in this letter were performed for the type II MOT; however, similar results have been obtained for the type I MOT.

To extract and dissociate the Na_2^+ ions from the trap the electrode configuration shown in figure 2 is used. Its design is similar to the electrode system described by Blangé *et al.* [10]. The electrodes E1 and E2 surrounding the atom cloud pull the Na_2^+ ions into the electrode system where they are subsequently accelerated up to 100 eV, and by means of the deflectors D1 and D2 and a lens L1 directed through the dissociating laser beam. In the dissociation volume typically a fraction 10^{-3} of the molecular ions is dissociated producing fragment ions with a kinetic energy of 40-60 eV in the lab frame. The spread in the kinetic energy is the result of the recoil energy released in the dissociation which is typically 0.65 eV in the center of mass frame. Electrostatic lens L2 focuses the ions and deflector D3 separates the fragment ions from the molecular ions and directs the Na^+ (or the Na_2^+) ions to the channel electron multiplier. Due to the transverse spread of the ions the detection efficiency η_{Na+} of the fragment ions will be smaller than the detection efficiency $\eta_{Na_2^+}$ of the Na_2^+ ions. To determine the absolute value of the photodissociation cross section only the ratio $\eta = \eta_{Na+}/\eta_{Na_2^+}$ is needed and this is estimated by comparing the signal of the narrow Na_2^+ image on the detector with the signal in the case of a Na_2^+ beam which is expanded by means of electrostatic lens L2 up to the expected size of the fragment ion image. We find $\eta \approx 0.57 \pm 0.11$. The uncertainty in this procedure mainly determines the uncertainty in the measurement of the absolute value of the photodissociation cross section.

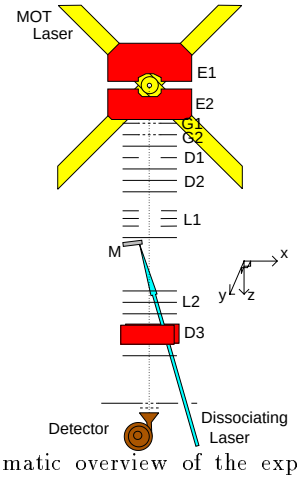

FIG. 2. Schematic overview of the experimental set-up. The dotted line in the electrode system represents a typical Na_2^+ ion trajectory. Note that the channel electron multiplier is placed off-axis.

Since the detection efficiencies do not change significantly during an experimental session (about 8 hours) the wavelength dependence of the cross section during a session is much better determined. It is only the wavelength dependence of the photodissociation yield which is needed in the determination of the vibrational state population. The experiment was completed in four measurement sessions, dividing the photodissociation spectrum in four wavelength regions provided by the dyes DCM (615-690nm), Rhodamine 590 (580-615nm), Pyrromethene (526-580nm) and by the spectral lines of the Ar^+ 5W pump laser (457-515nm). Using the measurements in the overlapping wavelength regions the Pyrromethene and the Rhodamine measurements were scaled to the DCM

measurements yielding corrections within 20%. Since the wavelength range of the Ar^+ laser does not have an overlap with the Pyrromethene dye range a rescaling factor was included as a free parameter in the data analysis.

As input for the data analysis we use the photodissociation cross section as a function of wavelength λ for the accessible ro-vibrational levels as calculated by Rudolph *et al.* [13] using *ab initio* potentials for Na_2^+. The $1^2\Sigma_u^+$ potential reached in the excitation from the $X^2\Sigma_g^+$ state is strongly repulsive, and the electronic transition moment is only a slowly varying function of the internuclear distance [13]. This results in a so-called reflection of the vibrational wavefunction of the initial state as a function of the wavelength of the dissociating laser, resulting in a form of the cross section resembling the ionic ground state vibrational wavefunction. The sum of the calculated cross sections $\sigma_v(\lambda)$ with the populations $P(v)$ of the vibrational states as weighting parameters is fitted to the measured total photodissociation yield $\sigma_{PD}(\lambda)$ according to

$$\sigma_{PD}(\lambda) = \sum_v P(v)\,\sigma_v(\lambda). \qquad (2)$$

Only the vibrational states with $v \leq 3$ are energetically accessible. For the extremely low collision energy available in this experiment the rotational excitation of the Na_2^+ ion is not high enough to influence significantly the photodissociation cross section [10]. For the final analysis a rotational state distribution was taken into account proportional to the degeneracy $2J+1$ of the rotational levels up to the energetically allowed maximum rotation quantum number J_{max} [9]. Fitting procedures assuming all rotational population in the $J=0$ states or in the maximum energetically attainable rotational state $J = J_{max}$ gave within $\pm 2\%$ the same vibrational state populations $P(v)$.

Figure 3 shows the measured photodissociation cross section as a function of the wavelength. The solid line represents a least-squares fit of the calculated spectrum to the experimental data with the relative populations $P(1) - P(3)$ and a rescaling factor for the wavelength range of the Ar^+ laser as free parameters. After normalization the resulting vibrational state distribution is $P(1)$=0.003±0.016, $P(2)$=0.291±0.022 and $P(3)$=0.706±0.022. In the experimental data the four maxima that are characteristic for the $v=3$ state are clearly present. The population of the $v=2$ state is clearly seen through the non zero photodissociation cross section at the three minima. The fact that out of four energetically allowed vibrational states only two are populated is strong evidence for the PAAI mechanism. It can furthermore be concluded that the active doubly excited molecular potential curve involved has to cross the $X^2\Sigma_g^+$ ground state potential of Na_2^+ close to the classical outer turning point of the $v=3$ state.

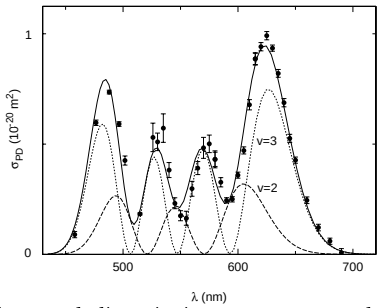

FIG. 3. Measured dissociation spectrum and least-squares fit (solid line) of the experimental data to the calculated spectrum. The dashed lines show the contributions of the various vibrational states to the fit. The error bars on the experimental data represent the statistical uncertainty. The systematic error in the absolute value of the cross sections is ≈ 20%.

To definitely rule out of the PAPI process we have calculated the branching ratios for the PAPI process, which is in the Franck-Condon approximation proportional to the overlap between the vibrational wavefunction of the singly excited intermediate state of Na_2 and that of the Na_2^+ electronic ground state. Long range states in the intermediate state such as the 0_g^- state previously identified [3,6] with a classical inner turning point of more than $50a_0$ lead to no appreciable Franck-Condon overlap, and do therefore not lead to PAPI. Short range states such as the 1_g state have, however, a significant vibrational overlap with all the lower vibrational levels of the electronic ionic ground state and could lead to PAPI. For example, the v=100 state of the 1_g state, which is only bound with 0.25 cm^{-1}, has relative branching ratios of 0.032, 0.263, 0.541, and 0.164 for transitions to the v=0–3 vibrational levels of the $X^2\Sigma_g^+$ state of Na_2^+, respectively. Similar Franck-Condon patterns are found for other highly excited vibrational levels of the 1_g state. This is to be expected, since the electronic part of the transition matrix element is a smooth and slowly varying function of the final electron energy and the internuclear distance [13]. Since this distribution is in clear disagreement with the measured distribution we can rule out the PAPI process as the main mechanism leading to ionization in ultra-cold collisions under the conditions in our experiment.

The dominance of the PAAI process over the PAPI process is ultimately determined by the different cross section for the two processes. Based on our recent calculations for photoionization from the ground state of Na_2 [13] and the cross sections for the associative ionization process [14] it is found that the PAAI process should be dominant if energetically allowed. This is in agreement with the earlier estimates of Macholm *et al.* [15] where the PAAI mechanism is also found to be dominant.

The uncertainty in $P(v)$ is determined solely by the discrepancy between the measurement and the theoretical calculation. As can be seen in Fig. 3 the experimental values tend to be displaced with respect to the theoret-

ical curve by a few nm. This discrepancy is also clear if we consider the reduced χ^2 of the fitting process, for which we expect a value close to 1 for a good fit, but which is 10.33 in our case. Inclusion of the $P(0)$ in the fitting procedure did not improve the reduced χ^2, nor did it influence significantly the population of the other states. It did lead to a slightly negative population of $P(0)$ which is unphysical. Therefore $P(0)$ was retained at 0. A shift in wavelength of 3 nm corresponds to a shift in the potential curves of only 10 meV or equivalently in a shift in the internuclear distance of only $0.015\,a_0$, which is well within in the accuracy of the *ab initio* calculated potential curves. This underlines that our method when applied to cold collisions is a very sensitive probe for the molecular potentials involved.

Previous measurements of the vibrational state population in Na_2^+ ions produced via associative ionization in a thermal beam have been reported at mean collision energies $E_c = 10$ meV and 25 meV, which are four orders of magnitude larger than in the MOT [9]. They also showed a pronounced population of $v = 3$ ($P(3)$=0.55 and 0.33, respectively). This indicates that the ionization process determining the ionic vibrational distribution in cold collisions occurs via the same molecular potential curve as in the associative ionization process at thermal energies.

Apart from the wavelength dependence of the photodissociation cross section, we can also make a comparison between experiment and theory for the absolute photodissociation cross section. At $\lambda = 630$ nm we measure a photodissociation cross section of $\sigma_{PD} = (0.95\pm0.13) \times 10^{-20}$ m^2, whereas the calculated cross section for this wavelength is 0.873×10^{-20} m^2 using the vibrational distribution given above. This agreement between theory and experiment is much better than in previous studies of the photodissociation cross sections of Na_2^+ [10,16], which report experimental cross section which are a factor two and three smaller than the theoretical predictions [17].

In summary, using our recently developed photodissociation method we have found that the vibrational energy distribution in Na_2^+ ions extracted from a sodium MOT is dominated by the population in the $v = 2$ (0.29 ± 0.02) and $v = 3$ (0.71 ± 0.02). These results agree with an extrapolation of results obtained in the low thermal regime with mean collision energies of 10 and 25 meV. The theoretical calculation of the photodissociation cross section via the $X^2\Sigma_g^+ \rightarrow 1^2\Sigma_u^+$ transition is confirmed by experiment, both in absolute value and the wavelength dependence. The high precision of the measurements provides a challenge to improve the theoretical calculations of the wavelength dependent photodissociation cross section even further. The obtained information on the molecular potential curve responsible for autoionization can be used to gain further insight in the dynamics and molecular symmetries involved in collisions between ultracold Na atoms. The application of our method in experiments with two-color excitations [6] allows for a control of the relevant excitation steps in the reaction mechanism and can, in this sense, be considered as a complete experiment on photo-assisted collisions between two sodium atoms in the cold collision regime.

This work has been supported by the "Stichting voor Fundamenteel Onderzoek der Materie (FOM)", which is financially supported by the "Nederlandse organisatie voor Wetenschappelijk Onderzoek (NWO)". This work has furthermore been partially supported by the European Union's Human Capital and Mobility Programme under contract number ERBCHRXCT930344.

---

* Present address: Département de Physique, Université Catholique de Louvain, Chemin du Cyclotron 2, B-1348 Louvain-la-Neuve, Belgium.

[1] T. Walker and P. Feng, Adv. At. Mol. Opt. Phys. **34**, 125 (1994).

[2] P.L. Gould, P.D. Lett, P.S. Julienne, W.D. Phillips, H.R. Thorsheim and J. Weiner, Phys. Rev. Lett. **60**, 788 (1988).

[3] P.D. Lett, K. Helmerson, W.D. Phillips, L.P. Ratliff, S.L. Rolston, and M.E. Wagshull, Phys. Rev. Lett. **71**, 2200 (1993).

[4] J.D. Miller, R.A. Cline, and D.J. Heinzen, Phys. Rev. Lett. **71**, 2204 (1993).

[5] L.P. Ratliff, M.E. Wagshull, P.D. Lett, S.L. Rolston, and W.D. Phillips, J. Chem. Phys. **101**, 2638 (1994).

[6] P.A. Molenaar, P. van der Straten, and H.G.M. Heideman, Phys. Rev. Lett. **77**, 1460 (1996).

[7] P.D. Lett, L.P. Ratliff, M.E. Wagshull, S.L. Rolston, and W.D. Phillips, in *Resonance Ionization Spectroscopy 1994*, H.-J. Kluge, J.E. Parks, and K. Wendt, Eds., AIP Conference Proceedings **329**, 289 (1995).

[8] E.L. Raab, M. Prentiss, A. Cable, S. Chu and D.E. Pritchard, Phys. Rev. Lett. **59**, 2631 (1987)

[9] J.J. Blangé, X. Urbain, H. Rudolph, H.A. Dijkerman, H.C.W. Beijerinck and H.G.M. Heideman, submitted to J. Phys. B, (1996)

[10] J.J. Blangé, X. Urbain, H. Rudolph, H.A. Dijkerman, H.C.W. Beijerinck and H.G.M. Heideman, J. Phys. B **29**, 2763 (1996)

[11] C. Monroe, W. Swann, H. Robinson, and C. Wieman, Phys. Rev. Lett. **65**, 1571 (1990)

[12] M. Prentiss, A. Cable, J.E. Bjorkholm, S. Chu, E. Raab, and D.E. Pritchard, Opt. Lett. **13**, 452 (1988)

[13] H. Rudolph and X. Urbain, Phys. Rev. A. **53**, 4111 (1996)

[14] O. Dulieu, S. Magnier, F. Masnou-Seeuws, Z. Phys. D **32**, 229 (1994)

[15] M. Macholm, A. Giusti-Suzor, F. Mies, Phys. Rev. A. **50**, 5025 (1994)

[16] A. Kortyna, D. Reisner, J. Unruh and L. Hüwel, Phys. Rev. A. **50**, 1399 (1994)

[17] The discrepancy between theory and experiment in ref. [10] is caused by overestimating the detection efficiency of the fragment ions by a factor three, which has been verified by numerical simulations of the trajectories of the fragment ions.